Supporting Information

Vanadium-cobalt oxyhydroxide shows ultralow overpotential for oxygen evolution reaction

Yan Cui,[a] Yuan Xue,[a] Rui Zhang,[a] Jian Zhang,*[b,c] Xing'ao Li,*[b,c] and Xinbao Zhu[d]

[a]Key Laboratory of Broadband Wireless Communication and Sensor Network Technology, Ministry of Educationy, Nanjing University of Posts and Telecommunications, Nanjing 210003, PR China

[b]New Energy Technology Engineering Lab of Jiangsu Province, School of Science, Nanjing University of Posts & Telecommunications (NUPT), Nanjing 210023, P. R. China. Email: iamjzhang@njupt.edu.cn; lxahbmy@126.com

[c]Key Laboratory for Organic Electronics and Information Displays & Institute of Advanced Materials (IAM), Jiangsu National Synergetic Innovation Center for Advanced Materials (SICAM), Nanjing University of Posts & Telecommunications, Nanjing 210023, P. R. China.

[d]College of Chemical Engineering, Nanjing Forestry University, Nanjing 210037, PR China.

Experimental Section

Chemicals. All the chemicals were of analytical grade, purchased from Aladdin Reagent Co. Ltd., and were used without further purification.

Synthesis of V doped CoOOH nanorods. In brief, 40 mL mixed aqueous solution consisting of $CoCl_2$ (0.08 M) and NaOH (0.2 M) was prepared, to which a given amount of NH_4VO_3 was added so that the Co/V atomic ratio in the solution was controlled as 1:0, 0.9:0.1, 0.8:0.2 and 0.7:0.3, denoted as CoOOH, $Co_{0.9}V_{0.1}OOH$, $Co_{0.8}V_{0.2}OOH$ and $Co_{0.7}V_{0.3}OOH$, respectively. Furthermore, 10 mM of hexamethyltetramine was added to above solutions. After 30 min of continuous stirring, the mixed solution was then transferred into a 50 mL Teflon-lined stainless steel autoclave and maintained at 150 ℃ for 12 h. After cool down to room temperature, the precipitate thus formed were collected, washed with hydrogen peroxide (20 wt %), deionized water and ethanol twice and freeze-dried for further use.

Characterizations. The X-ray diffraction (XRD) was carried out on a D8 Advance X-ray powder diffractometer with Cu Ka radiation with a scan speed of 0.5 s per step. The morphologies of the samples were characterized by transmission electron microscopy (TEM) (FEI Tecnai F20) at an acceleration voltage of 200 kV. Scanning transmission electron microscopy (STEM) was performed using a FEI Titan 80-200 (ChemiSTEM) electron microscope operated at 200 kV, equipped with a high angle annular dark field (HAADF) detector, while compositional maps were obtained with energy dispersive spectroscopy (EDS) using four large solid-angle symmetrical Si drift detectors. The scanning electron microscopy (SEM) images were obtained on a scanning electron microscope (Hitachi S-4800). The X-ray photoelectron spectra images (XPS) were performed on a ESCALAB 250Xi X-ray photoelectron spectrometer with Al Kα radiation. Raman measurements were performed on a Horiba XploRA Confocal Raman microscope fitted with 532 nm excitation laser. The BET surface area was measured using the nitrogen gas adsorption-desorption method (TriStar II 3020) at 77 K.

Electrochemical measurements. All the electrochemical measurements were performed in a standard three-electrode setup and recorded using an electrochemical workstation (CHI 660E). The sample ink was prepared by mixing the catalyst (1.0 mg), propanol, and Nafion (0.5 wt%, 20 μL) followed by sonication for 30 min. The working

electrode was prepared by decorating the Ni foam electrode with dispersion at a loading mass of ~0.2 mg cm^{-2}. Saturated calomel electrode and graphite rod were selected as the reference and counter electrode, respectively. 1 M KOH solution purged with nitrogen was used as the electrolyte. Linear sweep voltammograms (LSV) were measured at a scan rate of 5 mV s^{-1} with a 95% iR correction. Cyclic voltammograms were recorded at various scan rates (10, 20, 40, 60, 80, and 100 mV s^{-1}) to estimate the double-layer capacitance. All the potentials were calibrated to reversible hydrogen electrode (RHE). For comparison, the commercial IrO_2 catalysts (Sigma-Aldrich) were also tested with the same experiment conditions.

Computational details. Spin-polarized density functional theory (DFT) calculations were performed using the plane-wave technique and GGA-PBE functional,[1] as implemented in the VASP code.[2,3] The ion-electron interactions were described using the projector-a. CoOOH is the most stable phase of Cobalt oxide under oxygen evolution reaction conditions, and (104) is its most stable and active facets.[4] A 2×2 supercell was used, and the Brillouin zone is sampled by a 3×3 Monkhorst-Pack grid. One of the top layer Co atoms was substituted by V to present V doped CoOOH. To describe the transition metal elements, DFT+U[5] method have been used with the *ab initio* U values,[6] U – J = 3.3 eV for Co and U – J = 3.4 eV for V species. The structures were optimized (with the bottom three layers fixed) until the maxima force on the atoms was smaller than 0.02eV/Å.

$$* + OH^- \rightarrow *OH + e^- \quad \text{(S1)}$$

$$OH + OH^- \rightarrow *O + H_2O + e^- \quad \text{(S2)}$$

$$*O + OH^- \rightarrow *OOH + e^- \quad \text{(S3)}$$

$$*OOH + OH^- \rightarrow O_2 + H_2O + e^- + * \quad \text{(S4)}$$

where * denotes an adsorption site. The free energy change for the four steps ($\Delta G_{1\text{-}4}$) can be calculated using:

$$\Delta G_1 = \Delta G_{*OH} \quad \text{(S5)}$$

$$\Delta G_2 = \Delta G_{*O} - \Delta G_{*OH} \quad \text{(S6)}$$

$$\Delta G_3 = \Delta G_{*OOH} - \Delta G_{*O} \quad \text{(S7)}$$

$$\Delta G_4 = 4.92 - \Delta G_{*OOH} \quad \text{(S8)}$$

Where the adsorption free energy for adsorbates (ΔG_{ads}) can be obtained by the corresponding ΔE_{ads} with the ZPE and entropy corrections:

$$\Delta G_{ads} = \Delta E_{ads} + \Delta E_{ZPE} - T\Delta S \quad \text{(S9)}$$

The theoretical overpotentials (η) for OER can be estimated using the equations:

$$G^{OER} = \max\{\Delta G_1, \Delta G_2, \Delta G_3, \Delta G_4\}; \quad \text{(S10)}$$

$$\eta^t = G^{OER}/e - 1.23\ \text{V}. \quad \text{(S11)}$$

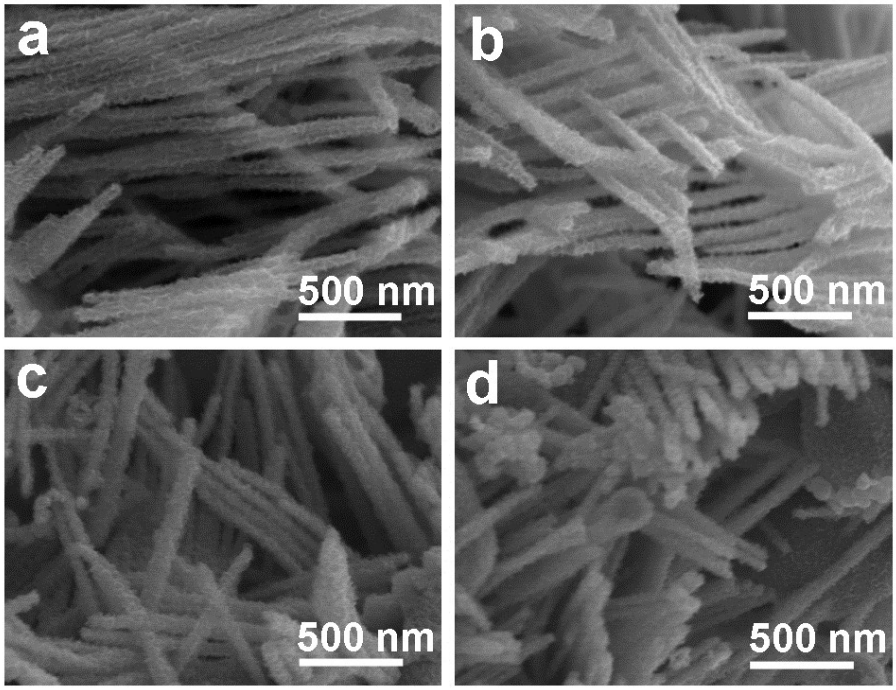

Fig. S1 SEM images of COOH (a), $Co_{0.9}V_{0.1}OOH$ (b), $Co_{0.8}V_{0.2}OOH$ (c) and $Co_{0.7}V_{0.3}OOH$ (d).

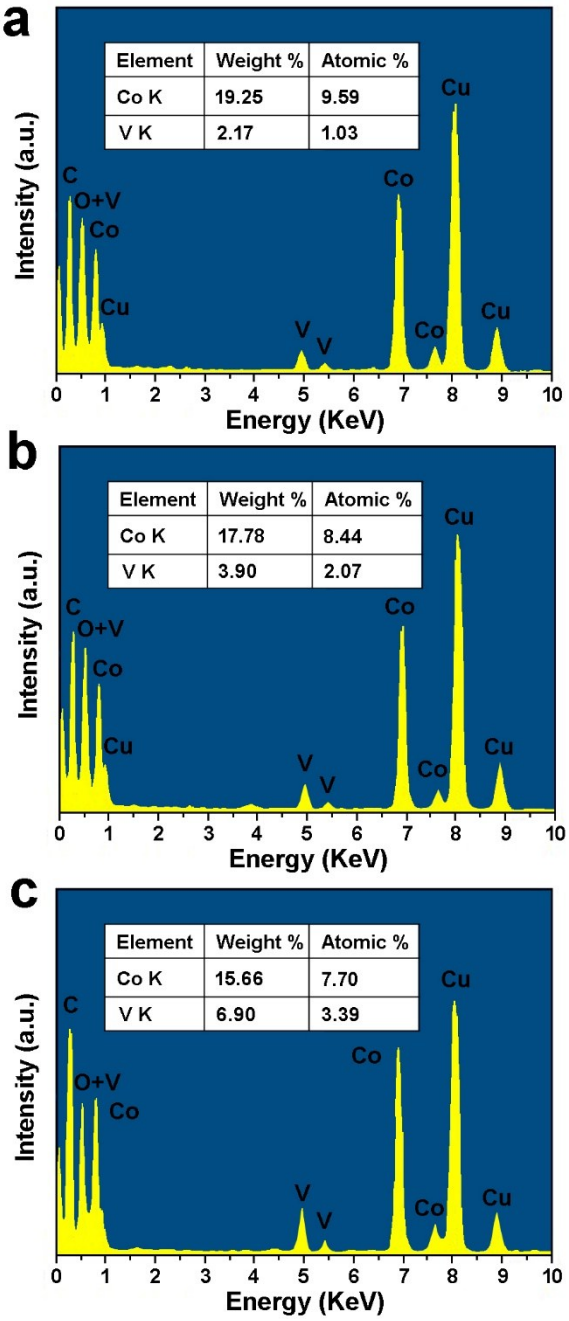

Fig. S2 EDX spectrum of $Co_{0.9}V_{0.1}OOH$ (a), $Co_{0.8}V_{0.2}OOH$ (b) $Co_{0.7}V_{0.3}OOH$ (c) samples.

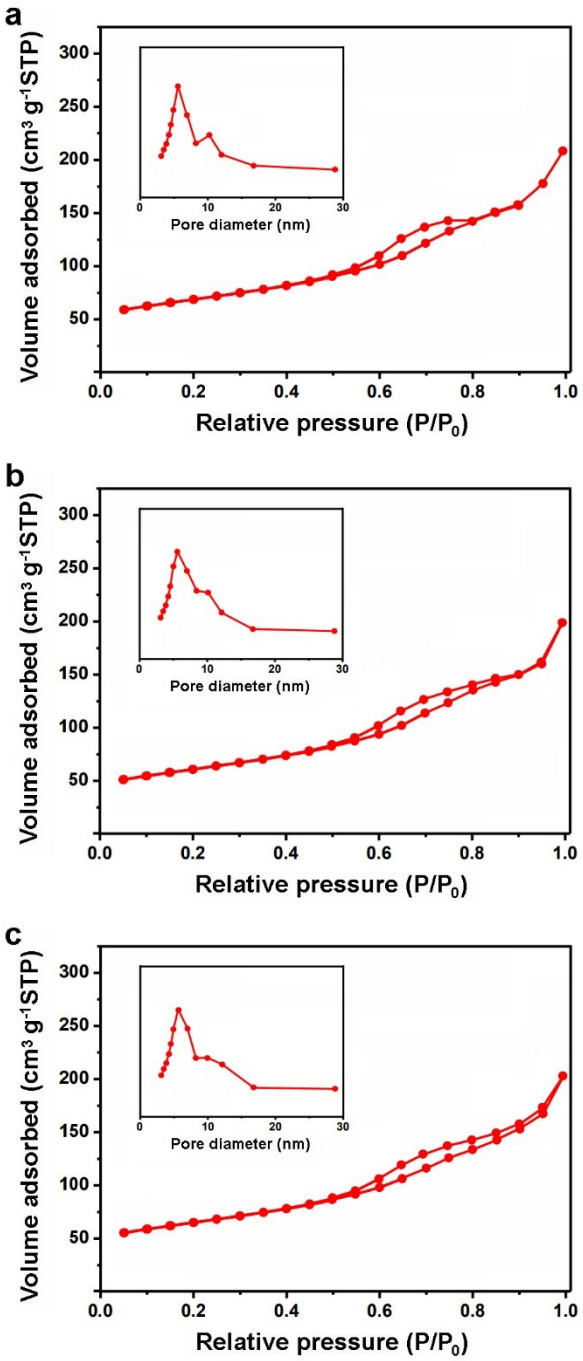

Fig. S3 N_2 adsorption-desorption isotherms with pore size distribution of CoOOH (a), $Co_{0.9}V_{0.1}OOH$ (b) and $Co_{0.7}V_{0.3}OOH$ (c).

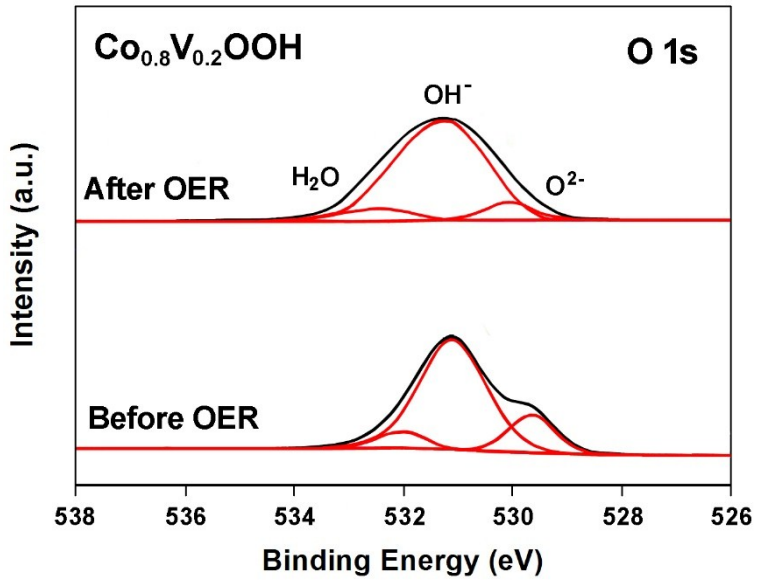

Fig. S4 O 1s XPS spectra of $Co_{0.8}V_{0.2}OOH$ before and after OER tests.

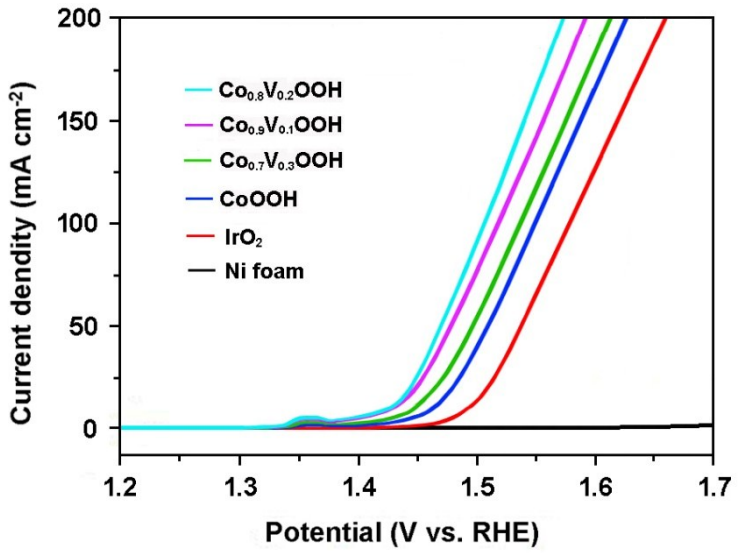

Fig. S5 Polarization curves for CoOOH, $Co_{0.9}V_{0.1}OOH$, $Co_{0.8}V_{0.2}OOH$, $Co_{0.7}V_{0.3}OOH$, IrO_2 and NF without iR correction.

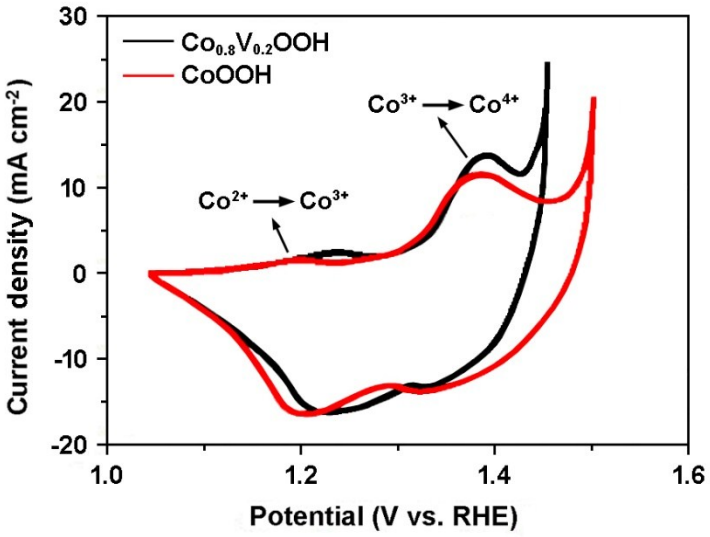

Fig. S6 Cyclic voltammetric curves of CoOOH and $Co_{0.8}V_{0.2}OOH$ recorded at a scan rate of 1 mV s^{-1}.

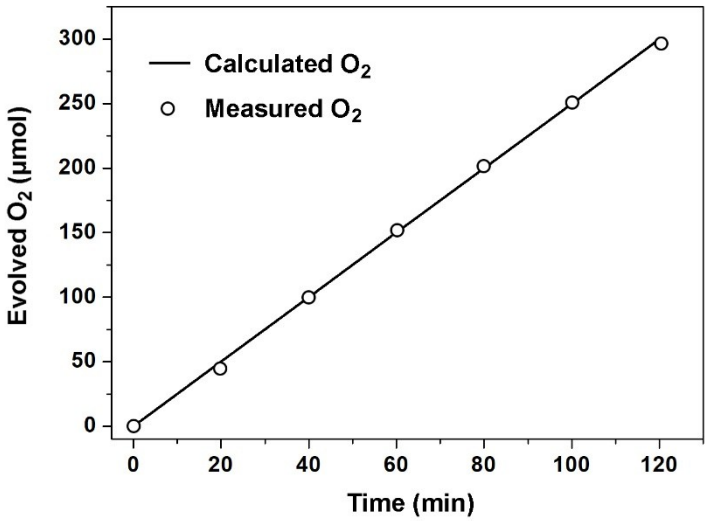

Fig. S7 Experimentally measured (applied potential of 1.45 V (vs RHE)) and theoretical amount of O_2 evolved during the OER for 120 min with $Co_{0.8}V_{0.2}OOH$ electrocatalyst.

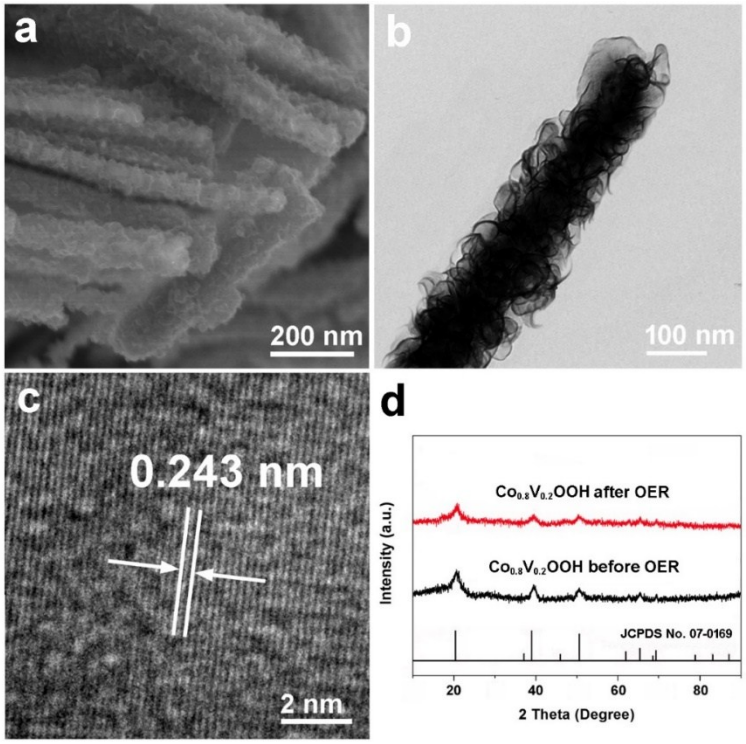

Fig. S8 SEM (a), TEM (b) HRTEM (c) and XRD (d) images of $Co_{0.8}V_{0.2}OOH$ after OER test.

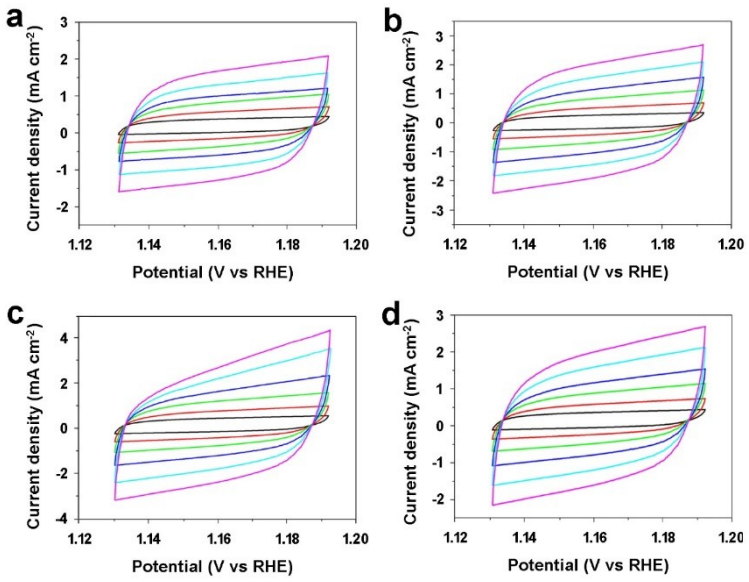

Fig. S9 Cyclic voltammetry curves in a nonfaradaic potential region under different scan rates of CoOOH based electrodes with the scan rates of 10, 20, 40, 60, 80 and100 $mV \cdot s^{-1}$. a: CoOOH, b: $Co_{0.9}V_{0.1}OOH$, c: $Co_{0.8}V_{0.2}OOH$ and d: $Co_{0.7}V_{0.3}OOH$.

Table S1. Comparison of OER activities for $Co_{0.8}V_{0.2}OOH$ with other metal oxide/(oxy)hydroxides/sulfide OER electrocatalysts in alkaline solutions.

Electrocatalysts	**Electrolyte**	**Mass loading**	***η* vs. 10 mA cm^{-2}**	**Ref**
VOOH	1 M KOH	0.80 mg cm^{-2}	1.55 V	7
$Fe_{0.5}V_{0.5}OOH$	1 M KOH	0.143 mg cm^{-2}	1.58 V	8
Ni-B@NiO_xH	1 M KOH	0.21 mg cm^{-2}	1.61 V	9
MoFe:$Ni(OH)_2$/NiOOH	1 M KOH	--	1.47 V	10
$Fe_{0.33}Co_{0.67}OOH$	1 M KOH	--	1.50 V	11
CeO_x/CoO_x	1 M NaOH	--	1.54 V	12
Co-V hydr(oxy)oxide	1 M KOH	0.2 mg cm^{-2}	1.48 V	13
F-CoOOH	1 M KOH	3.0 mg cm^{-2}	1.50 V	14
CoS_x/N-doped graphene	1 M KOH	0.21 mg cm^{-2}	1.56 V	15
Ni-Fe LDH	1 M KOH	0.13 mg cm^{-2}	1.44 V	16
Ni:FeOOH	1 M KOH	0.142 mg cm^{-2}	1.44 V	17
Se-FeOOH	1 M KOH	--	1.52 V	18
Fe-doped β-$Ni(OH)_2$	1 M KOH	--	1.45 V	19
MoS_2/FeOOH	1 M KOH	2.0 mg cm^{-2}	1.46 V	20
$Co_{0.8}V_{0.2}OOH$	**1 M KOH**	**0.2 mg cm^{-2}**	**1.42 V**	**This work**

Referances

1 J. Perdew, L. Burke and M. Ernzerhof, *Phys. Rev. Lett.*, 1996, **77**, 3865-3868.

2 G. Kresse and J. Hafner, *Phys. Rev. B*, 1993, **47**, 558.

3 G. Kresse and J. Furthmüller, *Comput. Mater. Sci*., 1996, **6**, 15-50.

4 M. Bajdich, M. Garcíamota, A. Vojvodic, J. K. Nørskov and A. T. Bell, *J. Am. Chem. Soc*., 2013, **135**, 13521.

5 S. Dudarev, G. Botton, S. Savrasov, C. Humphreys and A. Sutton, *Phys. Rev. B*, 1998, **57**, 1505

6 N. J. Mosey, P. Liao and E. A. Carter, *Phys. Rev. B: Condens. Matter*, 2008, **129**, 014103.

7 H. Shi, H. Liang, F. Ming and Z. Wang, *Angew. Chem. Int. Edit.*, 2017, **56**, 573-577.

8 K. Fan, Y. Ji, H. Zou, J. Zhang, B. Zhu, H. Chen, Q. Daniel, Y. Luo, J. Yu and L. Sun, *Angew. Chem. Int. Edit*., 2017, **56**, 3289-3293.

9 J. Masa, I. Sinev, H. Mistry, E. Ventosa, M. Mata, J. Arbiol, M. Muhler, B. Cuenya and W. Schuhmann, *Adv. Energy Mater*., 2017, **7**, 1700381.

10 Y. Jin, S. Huang, X. Yue, H. Du and P. Shen, *ACS Catal.*, 2018, **8**, 2359-2363.

11 S. Ye, Z. Shi, J. Feng, Y. Tong and G. Li, *Angew. Chem. Int. Edit.*, 2018, **57**, 2672-2676.

12 J. Kim, K. Shin, K. Kawashima, D. Youn, J. Lin, T. Hong, Y. Liu, B. Wygant, J. Wang, G. Henkelman and C. Mullins, *ACS Catal.*, 2018, **8**, 4257-4265.

13 J. Liu, Y. Ji, J. Nai, X. Niu, Y. Luo, L. Guo and S. Yang, *Energy Environ. Sci*., 2018, **11**, 1736-1741.

14 P. Chen, T. Zhou, S. Wang, N. Zhang, Y. Tong, H. Ju, W. Chu, C. Wu and Y. Xie, *Angew. Chem. Int. Edit*., 2018, **57**, 15471-15475.

15 K. Fan, H. Zou, Y. Lu, H. Chen, F. Li, J. Liu, L. Sun, L. Toney, M. Sui, and J. Yu, *ACS Nano*, 2018, **12**, 12369-12379.

16 C. Kuai, Y. Zhang, D. Wu, D. Sokaras, L. Mu, S. Spence, D. Nordlund, F. Lin, and X. Du, *ACS Catal*., 2019, **9**, 6027-6032.

17 M. Suryawanshi, U. Ghorpade, S. Shin, U. Suryawanshi, E. Jo and J. Kim, *ACS Catal.*, 2019, **9**, 5025-5034.

18 S. Niu, W. Jiang, Z. Wei, T. Tang, J. Ma, J. Hu, and L. Wan, *J. Am. Chem. Soc*., 2019, **141**, 7005-7013.

19 T. Kou, S. Wang, J. Hauser, M Chen, S. Oliver, Y Ye, J. Guo, and Y Li, *ACS Energy Lett.*, 2019, **4**, 622-628.

20 Y. Jin, S. Huang, X. Yue, H. Du and P. Shen, *ACS Catal.*, 2018, **8**, 2359-2363.